Eur. Phys. J. A **7**, 87–99 (2000)

THE EUROPEAN PHYSICAL JOURNAL A

EDP Sciences

Subbarrier heavy ion fusion enhanced by nucleon transfer

V.Yu. Denisov[1,2,a]

[1] Institute for Nuclear Research, Prospect Nauki 47, 252028 Kiev, Ukraine
[2] GSI-Darmstadt, Planckstrasse 1, 64291 Darmstadt, Germany (e-mail: denisov@clri6a.gsi.de)

Received: 23 August 1999 / Revised version: 30 September 1999
Communicated by P. Schuck

Abstract. We discuss a model for the description of subbarrier fusion of heavy ions which takes into account the coupling to the low-energy surface vibrational states and to the few-nucleon transfer with arbitrary reaction Q-value. The fusion reactions ^{28,30}Si+^{58,62,64}Ni, ^{40}Ca+^{90,96}Zr, ^{28}S+^{94,100}Mo, ^{58}Ni+^{64}Ni, ^{16,18,20,22,24}O+^{58}Ni and ^{28}Si+^{124,126,128,130,132}Sn are analyzed in detail. The model describes rather well the experimental fusion cross section and mean angular momentum for reactions between nuclei near the β-stability line. It is shown that these quantities are significantly enhanced by few-nucleon transfer with large positive Q-value. A shape independent parameterization of the heavy ion potential at distances smaller then the touching point is proposed.

PACS. 25.60.Je Transfer reactions – 25.60.Pj Fusion reactions – 25.70.Hi Transfer reactions – 25.70.Jj Fusion and fusion-fission reactions

1 Introduction

Heavy ion fusion reactions at energies below or near the Coulomb barrier have received considerable attention [1-36]. Recently many different mechanisms were discussed for the description of subbarrier fusion reactions as coupling to the low-energy excited states, nucleons transfer, deformation of ions or neck formation during barrier penetration [3-36]. Fusion cross sections are strongly enhanced at energies below barrier by the coupling to both the low-energy surface vibrational states [3-16,28-32] and the few-nucleon transfer channels [3-11,15-25,32,35]. Models which take into account the coupling to the low-energy surface vibrational states as well as to the few-nucleon transfer channels describe well the fusion cross section $\sigma_{\rm fus}(E)$ and mean angular momentum of compound nucleus $\langle L(E)\rangle$ for reactions between nuclei near the line of β-stability.

The coupling potentials between the ground state channel and channels connected with the low-energy vibrational states are well-known [1,3-16]. Therefore the theory of fusion cross section enhancement due to coupling to low-energy vibrational states is well developed. In contrast to this, the coupling potential for transfer channels as a rule is not known with good accuracy. This potential may be fixed by studying quasi-elastic transfer reactions. Unfortunately, experimental information on quasi-elastic transfer reactions often is not available. Therefore the description of fusion cross section enhancement due to transfer reactions is based on the fitting parameters. Moreover, the radial shape of the coupling potential for transfer channels has various forms in the different models. For example, the radial dependence of the transfer coupling potential is chosen in the forms $F\exp[\alpha(r-R_{12})]$ [3,14] or $F\exp[\alpha(r-R_{12})]/r$ [18], where F is a coupling constant, α is a constant related to the separation energy of transferred particles or is taken from systematics [14], r is the distance between the centre of mass of the ions, $R_{12}=R_1+R_2$, R_1 and R_2 are the radii of the ions. Sometimes the transfer coupling potential has a similar form as the coupling potential to the low-energy vibrational states [11,20,30]. The value of the transfer constant is not fixed a priori and sometimes is chosen by the fitting experimental data [16,21].

The simplified coupled-channel code CCFUS [13] is often used for the analysis of subbarrier fusion of heavy ions [3,7-9,21,30-33]. As pointed out by Landowne (see [7,30]) the CCFUS model overestimates the contributions of the transfer channels in the case of large positive Q-value of the transfer reaction.

Recently, by using radioactive ion beams an experimental possibility was available to study fusion reactions between a nucleus far from the line of β-stability [34]. The fusion reactions induced by such colliding systems may be strongly enhanced by transfer reactions with a large positive Q-value. Therefore it is necessary to develop a simple model describing fusion reactions that takes into account the coupling both to the low-energy surface vibrational states and to the transfer channels with their large positive Q-values.

[a] Permanent address: e-mail: denisov@kinr.kiev.ua

The direct solution of coupled reaction channel equations is a difficult numerical problem, see for example [20]. It is shown in [9] that the heavy ion fusion cross sections calculated with the "exact" microscopic code is in good agreement with the one obtained by using the CCFUS model [13], when transfer channels are not important. Therefore we consider the coupling to the low-energy surface oscillations during the fusion process in the same manner as in the CCFUS model. We treat the coupling to the transfer channels in the DWBA approximation [1], which describes well the quasi-elastic transfer reactions near barrier [35]. The nucleon transfer during the fusion reaction will be considered in the WKB approximation [37].

The probability of barrier penetration is determined by the action in the WKB approximation [37]. We consider that nucleon transfer takes place during barrier penetration. Therefore the action splits into three terms. The tunneling from the outer turning point to the distance $r_{\rm tr}$, where the transfer of a particle takes place, is described by the first term. The second term relates to the probability of the nucleon transfer process at the distance $r_{\rm tr}$ between the ions. The third term describes the tunneling from $r_{\rm tr}$ to the inner turning point. The enhancement of the subbarrier fusion reaction due to the nucleon transfer process has not been considered in such approximation.

We describe the probability of nucleon transfer by using the semiclassical model. This model does not employ a transfer coupling constant. Therefore in our model it is not necessary to know from other experimental data the value of the coupling constant related to transfer processes for the calculation of the subbarrier fusion cross section. In contrast to previous considerations our method is valid for arbitrary Q-values of the transfer the reaction.

Our model is discussed in detail in the Sect. 2. In Sect. 3 $\sigma_{\rm fus}(E)$ and $\langle L(E)\rangle$ are calculated within the proposed model and compared with experimental data for fusion reactions induced by nuclei located along the β-stability line. The fusion reaction cross section and mean angular momentum of the compound nuclei obtained in this model are analyzed in the case of fusion reactions between β-stable nuclei and nuclei near the neutron drip line in Sect. 4. Summary and conclusions are presented in Sect. 5.

2 Subbarrier heavy ion fusion enhanced by nucleon transfer

The system of coupled channel equations in the case of coupling to the low-energy vibrational states has the form [1,3-5,10,11,13,14]

$$\left[-\frac{\hbar^2}{2\mu_i}\frac{d^2}{dr^2}+\frac{\hbar^2\ell_i(\ell_i+1)}{2\mu_i r^2}+V(r)-Q_i-E\right]\varphi_i(r) = -\sum_j V_{ij}(r)\varphi_j(r), \quad (1)$$

where $\psi_i(r)=\varphi_i(r)/r$ is the wave function, μ_i is the reduced mass, ℓ_i is the value of the orbital momentum in units of $\hbar$, $V(r)$ is the ion-ion interaction potential, Q_i is the Q-value of the reaction in channel i, E is the collision energy and $V_{ij}(r)$ is the coupling potential. The coupling potential between the ground state and the channels connected with the low-energy surface vibrational state of multipolarity λ is given by [1,3-5,10,11,13]

$$V_{0i}=\frac{\beta_i R_i}{\sqrt{4\pi}}\left[\frac{dV_{\rm i-i}(r)}{dr}+\frac{3}{2\lambda+1}\frac{z_1 z_2 e^2 R_i^{\lambda-1}}{r^{\lambda+1}}\right]. \quad (2)$$

Here $V_{\rm i-i}(r)$ is the nuclear part of the ion-ion interactions $V(r)$, z_1 and z_2 are the proton numbers, e is the proton charge and $\beta_i R_i$ is the deformation length of the i-th vibrational state in the nucleus with radius R_i.

As in [3,4,10,11,13,14] we propose that all reduced masses μ_i and orbital momenta ℓ_i are equal in all channels related to vibrational excitations. Then by taking the radial dependence of the coupling potential at the barrier position $V_{ij}(r)=V_{ij}(\overline{R})$ we diagonalize the system (1) with the help of the substitution

$$\varphi_i(r)=\sum_k U_{ik}\xi_k(r), \quad (3)$$

where U_{ik} is the transformation matrix and $\xi_k(r)$ is the wave function (eigenvector). The coupling matrix $\mathcal{M}_{ij}$ takes the form

$$\sum_{ij} U_{ki}\mathcal{M}_{ij}U_{jl}=\sum_{ij}U_{ki}[-Q_i\delta_{ij}+V_{ij}(\overline{R})]U_{jl}=\epsilon_k\delta_{kl} \quad (4)$$

and upon diagonalization we find the eigenvalue ϵ_k. In this case the partial fusion cross section $\sigma(E,\ell)$ is equal to [3,5,10,11,13-14]

$$\sigma(E,\ell)=\frac{\pi\hbar^2}{2\mu E}(2\ell+1)\sum_k |U_{k0}|^2 T(E,\mathcal{V}_{\ell k}), \quad (5)$$

where $T(E,\mathcal{V}_{\ell k})$ is the transmission coefficient obtained for the one-dimensional effective potential $\mathcal{V}_{\ell k}$

$$\mathcal{V}_{\ell k}(r)=V_\ell(r)+\epsilon_k=V(r)+\hbar^2\ell(\ell+1)/(2\mu r^2)+\epsilon_k. \quad (6)$$

We conclude from (5) that the partial cross section for fixed E and ℓ is determined by the sum of the transmission coefficients $T(E,\mathcal{V}_{\ell k})$ obtained for the effective potential $\mathcal{V}_{\ell k}$ with the weights $|U_{k0}|^2$. The effect of fusion cross section enhancement due to the coupling to the low-energy vibrational states is related to the smallest eigenvalue ϵ_k, which is negative.

The total fusion cross section is equal to

$$\sigma_{\rm fus}(E)=\sum_\ell \sigma(E,\ell). \quad (7)$$

Let us consider the transfer reaction in the DWBA approach, which described well nucleon transfer reactions near and below barrier [1]. In the DWBA approximation we neglect the influence of the transfer channels on the channels without transfer and on other transfer channels.

In this case the matrix $\mathcal{M}$ has a box structure. Each box of the matrix $\mathcal{M}$ in (4) is similar to the respective box without transfer. For each transfer channel we have an enhancement described by (4)–(6). For the sake of simplicity we propose that the values of ϵ_k and $|U_{k0}|^2$ for each specific transfer channel do not differ much from the ones obtained in (4) without transfer. Our proposal is based on a small variation of both the energies and the deformation lengths of the vibrational states in heavy nuclei which differ by several nucleons. In this case the partial fusion cross section in the transfer channel f is determined also by (4)–(6), but the transmission coefficient should be calculated by taking into account the few-nucleon transfer.

If the energy of collision is smaller than the barriers of the effective potentials before and after nucleon transfer and if the transfer occurred at the distance $r_{\rm tr}$, then the transmission coefficient may be written as

$$T(E,\mathcal{V}^i_{\ell k},\mathcal{V}^f_{\ell k})=1/\{1+\exp[\mathcal{A}(E,\mathcal{V}^i_{\ell k},\mathcal{V}^f_{\ell k},r_{\rm tr})]\}, \quad (8)$$

where the action $\mathcal{A}(E,\mathcal{V}^i_{\ell k},\mathcal{V}^f_{\ell k},r_{\rm tr})$ is given by

$$\mathcal{A}(E,\mathcal{V}^i_{\ell k},\mathcal{V}^f_{\ell k},r_{\rm tr})=\mathcal{A}^i(E,\mathcal{V}^i_{\ell k},r_{\rm tr})+\mathcal{A}^{\rm tr}(E,r_{\rm tr}) +\mathcal{A}^f(E,\mathcal{V}^f_{\ell k},r_{\rm tr}). \quad (9)$$

The action

$$\mathcal{A}^i(E,\mathcal{V}^i_{\ell k},r_{\rm tr})=(2/\hbar)\int_{r_{\rm tr}}^{r^i_{\ell k}}\sqrt{2\mu_i(r)(\mathcal{V}^i_{\ell k}(r)-E)}dr, \quad (10)$$

describes the tunneling of ions in an effective potential before nucleon transfer $\mathcal{V}^i_{\ell k}$ from the outer turning point $r^i_{\ell k}$ up to $r_{\rm tr}$, the action $\mathcal{A}^f(E,\mathcal{V}^f_{\ell k},r_{\rm tr})$

$$\mathcal{A}^f(E,\mathcal{V}^f_{\ell k},r_{\rm tr})=(2/\hbar)\int_{r^f_{\ell k}}^{r_{\rm tr}}\sqrt{2\mu_f(r)(\mathcal{V}^f_{\ell k}(r)-E)}dr \quad (11)$$

is related to the tunneling of ions in an effective potential after nucleon transfer $\mathcal{V}^f_{\ell k}$,

$$\mathcal{V}^f_{\ell k}(r)=V^f_\ell(r)+\epsilon_k-Q^f_{\rm tr} \quad (12)$$

from the point $r_{\rm tr}$ to the inner turning point $r^f_{\ell k}$ of the effective potential $\mathcal{V}^f_{\ell k}(r)$. Here $Q^f_{\rm tr}$ is the Q-value of the transfer reaction in the channel f.

In the case of m-neutron transfer during barrier penetration in fusion of heavy ions the action $\mathcal{A}^{\rm tr}(E,r_{\rm tr})$ connected with the nucleon transfer process may be written as

$$\mathcal{A}^{\rm tr}(E,r_{\rm tr})=(2/\hbar)\sum_{i=1}^{m}\sqrt{2M\mathcal{E}_i}(r_{\rm tr}-R_{12}-\delta) =2\alpha(r_{\rm tr}-R_{12}-\delta). \quad (13)$$

This form of the action describes the tunneling of m neutrons between spherical square potential wells of the colliding ions. In (13) we introduced a parameter δ because due to the finite diffuseness of the realistic nucleon-nucleus potential the barrier for the transferred nucleon disappears at the finite distance $\delta>0$ between the surfaces of the ions. The action similar to (13) is often used for the description of subbarrier neutron transfer reactions between heavy ions [1,35,39-44].

The wave function of the transferred nucleon may concentrate more in the volume or in the surface part of the nucleus. Due to this the nucleon transfer amplitude related to the overlap integral of the wave functions can have its maximum of transfer probability at relatively larger or smaller distances between colliding ions. It is possible to take into account this fine effect by a small variation of the parameter δ in (13).

The distance $r_{\rm tr}$ at which the nucleon transfer takes place is determined from the principle of minimal action, see Appendix and [37]. The trajectory of tunneling obtained by taking into account the few-nucleon transfer between heavy ions has its minimum value of the action (9) and its maximum value of the transmission coefficient (8). The few-nucleon transfer is especially important when $Q^f_{\rm tr}\gg 1$ MeV and the action (11) is small.

Note that the detailed derivation of (8)–(11), (13) by using the path integral is given in Appendix. These expressions can be also obtained by using the Landau method of complex classical paths for transitions in systems with arbitrary degrees of freedom, see for details (52.1) in [37].

The action $\mathcal{A}(E,\mathcal{V}^i_{\ell k},\mathcal{V}^f_{\ell k},r_{\rm tr})$ is a function of the Q-value of the transfer reaction and of the separation energies $\mathcal{E}_i$ of the transferred nucleons. Therefore the most favorable condition for the enhancement of subbarrier fusion due to few-nucleon transfer takes place at small separation energies of the transferred nucleons $\mathcal{E}_i$ and at large positive Q-values of the transfer reactions.

The expression (8) for the transmission coefficient is valid for collision energies E smaller than the effective barriers $\overline{\mathcal{V}}^i_{\ell k}$, before and $\overline{\mathcal{V}}^f_{\ell k}$, after the few-nucleon transfer. In the case $\overline{\mathcal{V}}^f_{\ell k}<E<\overline{\mathcal{V}}^i_{\ell k}$ and $r_{\rm tr}>\overline{R}^f_{\ell k}$ the transmission coefficient has the form

$$T(E,\mathcal{V}^i_{\ell k},\mathcal{V}^f_{\ell k})=1/\{1+\exp[\mathcal{A}^i(E,\mathcal{V}^i_{\ell k},r_{\rm tr}) +\mathcal{A}^{\rm tr}(E,r_{\rm tr})]\}\ T_{\rm HW}(E,\mathcal{V}^f_{\ell k}). \quad (14)$$

Here $\overline{R}^f_{\ell k}$ is the barrier distance of the effective potential $\mathcal{V}^f_{\ell k}$, $T_{\rm HW}(E,\mathcal{V}^f_{\ell k})$ is the transmission coefficient of the effective barrier after transfer obtained in the Hill-Wheeler approximation [45] and taking into account the reflection during barrier penetration. The subbarrier tunneling of ions before the nucleon transfer and the subbarrier nucleon transfer are described by the first factor in (14). The second factor in (14) is related to the transmission above the barrier between the ions after nucleon transfer.

If $\overline{\mathcal{V}}^f_{\ell k}<E<\overline{\mathcal{V}}^i_{\ell k}$ and $r_{\rm tr}<\overline{R}^f_{\ell k}$, then we should take into account the decay of the system after the few-nucleon transfer. In this case the transmission coefficient may be written as

$$T(E,\mathcal{V}^i_{\ell k},\mathcal{V}^f_{\ell k})=1/\{1+\exp[\mathcal{A}^i(E,\mathcal{V}^i_{\ell k},r_{\rm tr})+\mathcal{A}^{\rm tr}(E,r_{\rm tr})]\} \times(1-T_{\rm HW}(E,\mathcal{V}^f_{\ell k})). \quad (15)$$

At the high collision energy $E > \overline{\mathcal{V}}^f_{\ell k}$ and $E > \overline{\mathcal{V}}^i_{\ell k}$ we use the transmission coefficient in the Hill-Wheeler approximation. The corresponding modification of (14) and (15) are direct in this case. The expressions (8)-(13) are valid for the both positive and negative Q-values. The expressions (14)-(15) are valid for the case $Q_{\rm tr} > 0$ and may easily be transformed to the case $Q_{\rm tr} < 0$.

Nucleon transfer depends on the kinematic conditions related to Q-value preference of the heavy ions transfer reactions [1,15,35,38,39]. This kinematic conditions are described by the Gaussian-shape function [15,35,38,39]

$$F(Q) = \exp\left(-((Q_{\rm tr} - Q_{\rm opt})/\Gamma)^2\right), \qquad (16)$$

where $Q_{\rm opt}$ is the optimum Q-value of the transfer reaction and Γ is the width of Q window

$$\Gamma = 2\hbar\left(\frac{\alpha(2E - V(\overline{R}))}{\mu\overline{R}}\right)^{1/2}. \qquad (17)$$

Here the $V(\overline{R})$ and $\overline{R}$ are the value and the position of the barrier respectively, α is the asymptotic slope of the nucleon wave function far from the nucleus (see (13) for details). Function (16) describes well the experimental features of transfer reactions near barrier [35,39,40]. The optimum Q-value is close to zero for neutron transfer [1,35].

Let us consider the compound nucleus formed in transfer channel f with the ground state Q-value $Q^f_{\rm gg}$. The nucleon may also transfer to excited states [15]. Therefore the fusion cross section enhanced by the coupling to the transfer channel f and to the low-energy surface vibrations is equal to

$$\begin{aligned}\sigma^f_{\rm fus}(E) &= \sum_\ell \sigma^f_{\rm fus}(E,\ell) \\ &= \frac{\pi\hbar^2}{2\mu E}\sum_\ell (2\ell+1)\sum_k |U_{k0}|^2 \\ &\times \int_{-\infty}^{Q^f_{\rm gg}} dQ_{\rm tr}\ T(E,\mathcal{V}^i_{\ell k},\mathcal{V}^f_{\ell k})\ F(Q_{\rm tr})\ g(Q_{\rm tr}), \qquad (18)\end{aligned}$$

where $g(Q_{\rm tr})$ is the level density. Due to sharp exponential dependence of the transmission coefficient we may limit the integral in (18) to the range from ≈-10-15 MeV to $Q^f_{\rm gg}$ or even shorter and neglect the dependence of $g(Q_{\rm tr})$ on $Q_{\rm tr}$. We apply the value of level density at the Fermi surface $g(Q_{\rm tr}) = g_F = (6/\pi^2)g(N) = 6N/(\pi^2 a_g i)$ [15,46], where N is the number of neutrons in the ion that accepts i neutrons during transfer, $g(A) = A/a_g$ is the parameter of level density used in statistical model [46] and A is the number of nucleons in the nucleus. The compilation of the empirical values of parameter $g(A)$ is presented for some nuclei in [47].

Note that the value of Q-window width Γ is rather large (as a rule several MeV [1,35,39,40]), therefore the enhancement of heavy ion fusion due to neutron transfer is very important.

Equation (18) is valid under the assumption that the total flux of incident channel is going into this particular transfer channel. The other transfer channels and channels without transfer also give contributions into the fusion cross section. The incident channel flux is divided between the different channels. Therefore the total cross section is written as

$$\sigma_{\rm fus}(E) = \sum_{f,\ell} W_f(E,\ell)\sigma^f_{\rm fus}(E,\ell). \qquad (19)$$

Here

$$W_f(E,\ell) = \frac{P_f(E,\ell)}{\sum_f P_f(E,\ell)}, \qquad (20)$$

is the weight of transfer channel f in the total fusion cross section and

$$\begin{aligned}P_f(E,\ell) &= \sum_k |U_{k0}|^2 \\ &\times \int_{-\infty}^{Q^f_{\rm gg}} dQ_{\rm tr}\ T(E,\mathcal{V}^i_{\ell k},\mathcal{V}^f_{\ell k})\ F(Q_{\rm tr})\ g(Q_{\rm tr})\end{aligned}$$

is the coefficient relating to the probability of transfer channel f. Note that channels without transfer are also accounted for in (19)-(20) with factor $P(E,\ell) = \sum_k |U_{k0}|^2 T(E,\mathcal{V}^i_{\ell k})$.

In the case of m neutron transfer with Q-value $Q_{\rm tr}$ we proposed that every neutron is transferred with the same Q-value $Q_{\rm tr}/m$ and the factor $F(Q)$ in (18) and (20) is the product of single-neutron factor $F(Q)$ (16).

Note that the contributions of the channels with $Q_{\rm tr} \approx 0$ to the total cross section are small and negligible for $Q_{\rm tr} << -1$ MeV due to the exponential dependence of the transmission coefficient in the actions. Here we are not consider special cases when the transferred particle(s) exchanged between identical nuclei as in the cases of ^{12}C+^{13}C [20] or ^{58}Ni+^{60}Ni.

Now we determine the interaction potential between two ions at distance r,

$$V(r) = z_1 z_2 e^2/r + V_{\rm i-i}(r). \qquad (21)$$

Many different parameterizations of the nuclear interaction potential $V_{\rm i-i}(r)$ between spherical ions [1-7,47] are available. We choose the Krappe-Nix-Sierk $V_{\rm KNS}(r)$ [48] potential in our calculation for $r \geq R_{12} = R_1 + R_2$. The potential $V_{\rm KNS}(r)$ and the Coulomb energy depend on the shape of the ions at $r < R_{12}$. We would like to avoid a shape dependence of the potential $V(r)$. Hence we use a parameterization of the interaction potential $V(r)$ for $r < R_{12}$ in the form

$$V_{\rm fus}(r) = -Q_{\rm fus} + x^2(c_1 + c_2 x), \qquad (22)$$

where $Q_{\rm fus}$ is the Q-value of the fusion reaction obtained by using the mass table [49] or by using the mass formula [50], $x = (r - R_{\rm fus})/(R_{12} - R_{\rm fus})$, $R_{\rm fus}$ is the distance between the centers of mass of the left and right parts of the spherical compound nuclei. The coefficients c_1 and c_2 are obtained by matching at the touching point $R_{12} = R_1 + R_2$ for the potentials $V(r)$ (17) and $V_{\rm fus}(r)$ (18) and for its derivatives. We propose a quadratic dependence of $V_{\rm fus}(r)$

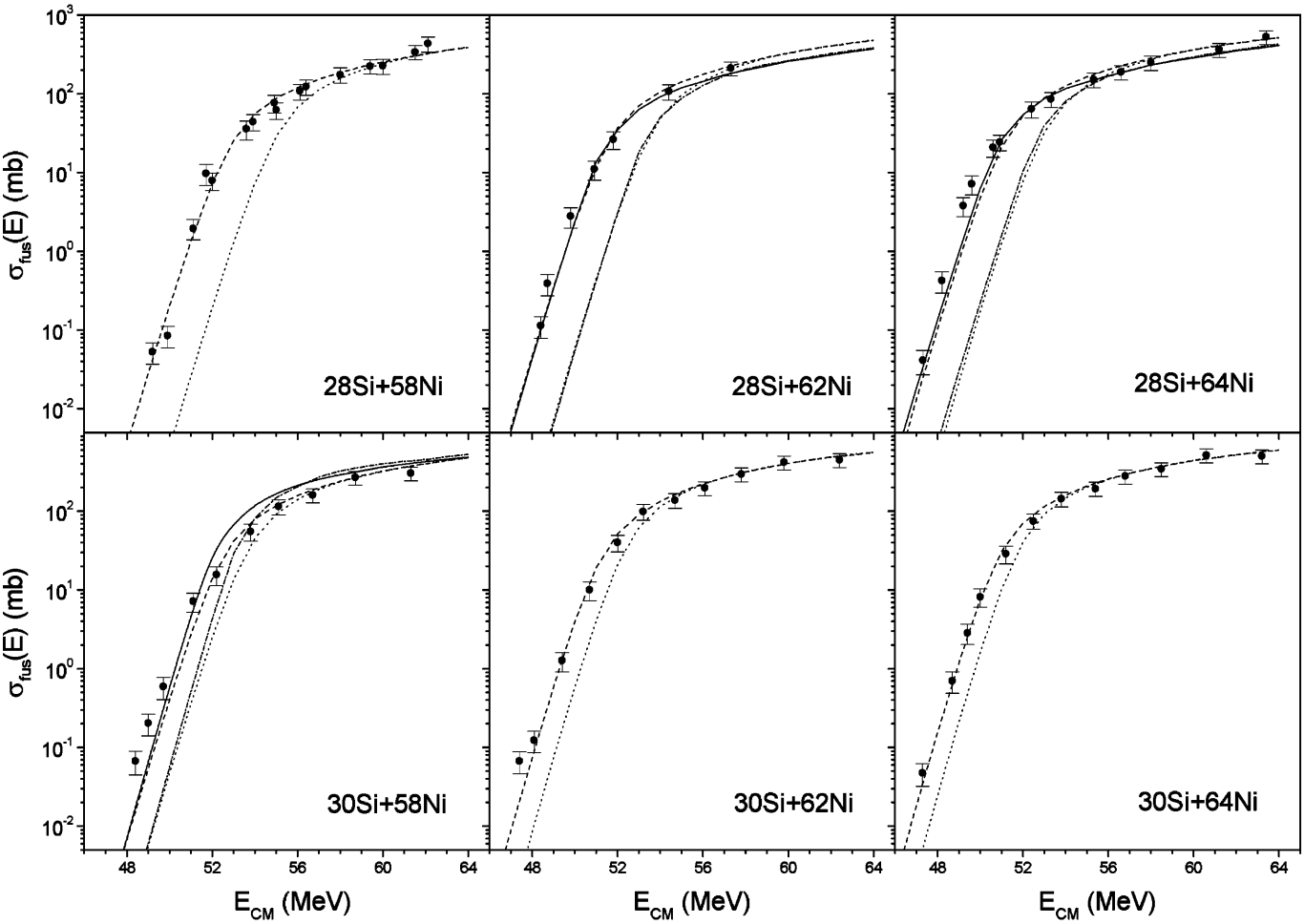

Fig. 1. Fusion cross sections for the reactions ^{28}Si+^{58,62,64}Ni (top) and ^{30}Si+^{58,62,64}Ni (bottom). Experimental data (dots) are taken from [31]. The results of the calculation taking into account both the low-energy 2^+ and 3^- states and the neutrons transfer channels are shown by the solid curves. The results of the calculation taking into account the coupling to the low-energy 2^+ and 3^- states are marked by the dash curves. The dash-dots curves correspond to the calculation with transfer channels only and the results of the calculation in the one-dimensional WKB approach are shown by dotted curves

at the point $x = 0$ because the potential (deformation) energy of the highly excited compound nucleus is minimum for the spherical shape, i.e. at $x = 0$.

The reduced mass μ for $r > R_{12}$ is determined by using a standard expression, see for example [1]. The reduced mass in (10) and (11) for $r < R_{12}$ is a function of r. We used the parameterization of $\mu(r)$ introduced in [51]

$$\mu_{i(f)}(r) = \mu_{i(f)}\{(17/15)\ k[(R_{12} - r)/(R_{12} - R_{\rm fus})]^2 \times \exp[-(32/17)\ (r/R_{\rm fus} - 1)] + 1\}, \qquad (23)$$

where $k = 16$ [51]. This semi-empirical dependence of the reduced mass is successfully used in the calculation of the lifetime of heavy nuclei for fission [51] and cluster [52] decays.

Note that if we neglect the influence of the transfer channels then the treatment of enhancement of coupled channels due to the low-energy excitations in our model is similar to the CCFUS model [13]. In this case the difference between our model and the CCFUS model is related to the calculation of the transmission coefficient below barrier. Below barrier this coefficient is estimated in the CCFUS model by using the Hill-Wheeler approximation [45] but we use the WKB approximation instead and obtain this coefficient by using the action. (Here we neglected the difference related to the parameterization of the nuclear part of the ion-ion potential because the calculations in both models can be done for the same parameterization of the nuclear potential.) Hence, if we neglect transfer channels our and the CCFUS models lead to similar results.

3 Entrance channel effects at fusion reactions

Let us consider several fusion reactions between nuclei located near the line of β-stability.

First we study isotopic effects in the fusion reactions ^{28,30}Si+^{58,62,64}Ni. The fusion cross sections calculated in different approaches for these reactions are compared with the experimental data [31] in Fig. 1. The one-dimensional tunneling model strongly underestimates the experimental

Table 1. Excitation energies E_ℓ, deformation parameters β_ℓ and multipolarities ℓ of the low-energy surface vibrational states, the values of the parameter r_0 in the $V_{\rm KNS}(r)$ nuclear potential [47] and the values of level density parameter a_g

Nucleus	E_2 (MeV)	β_2	E_3 (MeV)	β_3	r_0 (fm)	a_g (MeV)
^{16}O	6.92	0.36	6.13	0.60	1.21	10.37
^{18}O	1.98	0.39	5.10	0.48	1.21	10.37
^{20}O	1.63	0.39	5.62	0.48	1.21	10.37
^{28}Si	1.78	0.41	6.88	0.39	1.165	11.81
^{30}Si	2.24	0.22	5.59	0.15	1.20	12.55
^{40}Ca	3.90	0.11	3.74	0.34	1.21	11.43
^{58}Ni	1.45	0.18	4.47	0.22	1.18	13.62
^{62}Ni	1.17	0.22	3.76	0.14	1.19	10.33
^{64}Ni	1.34	0.17	3.56	0.15	1.20	10.19
^{90}Zr	2.19	0.08	2.75	0.14	1.21	12.66
^{96}Zr	1.76	0.12	1.91	0.22	1.23	11.43
^{94}Mo	0.87	0.128	2.53	0.161	1.175	10.12
^{100}Mo	0.534	0.226	1.91	0.21	1.185	8.21
^{124}Sn	1.13	0.076	2.59	0.072	1.18	10.42
^{126}Sn	1.14	0.076	2.72	0.072	1.18	10.52
^{128}Sn	1.17	0.076	2.76	0.072	1.18	10.62
^{130}Sn	1.22	0.076	2.49	0.072	1.18	10.71
^{132}Sn	1.22	0.076	2.49	0.072	1.18	10.81

fusion cross sections for the reactions ^{28,30}Si+^{58,62,64}Ni, see Fig. 1. We obtain similar results if neutron transfer channels with positive Q-value are taken into account, see Fig. 1. We describe well the experimental fusion cross sections for these reactions when the coupling to the low-energy 2^+ and 3^- surface excitation states is taken into account. However, we obtain better agreement with the experimental data for the reactions ^{28}Si+^{62,64}Ni and ^{30}Si+^{58}Ni when the coupling to the low-energy vibrational states and to the neutron transfer channels is taken into account simultaneously, see Fig. 1.

In our calculations we are taking into account 1-, 2-, 3- and 4-neutron transfer channels with positive Q-values. The Q-values of transfer reactions are obtained by using the mass table [49]. The Q-values of neutron transfer reactions for reactions ^{28}Si+^{62,64}Ni and ^{30}Si+^{58}Ni are small. Here and below we can neglect transfer channels with negative Q-value, because the influence of these channels is negligible. The energies and the deformation parameters of 2^+ and 3^- vibrational states were taken from other experimental data, see in [31,53]. These parameters are listed in Table 1. Here and below for the sake of fitting the experimental fusion cross section at high energies for these reactions we slightly change the parameter of the nuclear radii r_0 ($R_i = r_0 A_i^{1/3}$) in the KNS potential [48]. The values of r_0 used in our calculations are also given in Table 1. The values of r_0 for the Si and Ni in Table 1 insignificantly differ from $r_0 = 1.18$ fm recommended in [48]. We have done the calculation of the action (13) for $\delta = 0.7$ fm. This value of δ is reasonable, because it should be close to the value of the diffuseness of the realistic nucleon-nucleus potential.

We determine the value of statistical level density parameter $g(A)$ by using compilation [47]. When the value of $g(A)$ is not available in the compilation [47], we evaluate the value of $g(A)$ by using linear interpolation from nearest isotope(s). Note that nuclei close to double magic have very small level density [46,47]. Due to this we use somewhat larger value $a_g = 13.62$ MeV for isotope ^{58}Ni then that evaluated by using linear interpolation, 12.62 MeV. The values of a_g ($a_g = A/g(A)$) for nuclei considered here is listed in Table 1.

The nuclei ^{62,64}Ni and ^{30}Si are donors of neutrons in the reactions ^{28}Si+^{62,64}Ni and ^{30}Si+^{58}Ni. The fusion cross sections in collision of ^{28}Si with Nickel isotopes are enhanced with increasing the number of neutrons in Ni. Note that the same compound nucleus is formed in the fusion reactions ^{28}Si+^{64}Ni and ^{30}Si+^{62}Ni, but the fusion cross section for the former reaction is larger than for the latter due to the different values of the parameters of the 2^+ and 3^- surface vibrational states (see in Table 1) and the various contributions of the transfer channels.

The quality of description of the experimental fusion cross sections for the reactions Si+Ni in Fig. 1 in our model is similar to the one obtained by using the CCFUS model in [31]. This means that both models lead to similar results for transfer with the small Q-values.

Now we consider fusion reactions with large Q-values in the neutron transfer channels.

The fusion cross sections of ^{40}Ca+^{90,96}Zr [22] have been measured recently. The Q-values of 2- and 4-neutron transfer from ^{96}Zr to ^{40}Ca are equal to 5.526 MeV and 9.637 MeV respectively. In contrast to this the reaction ^{40}Ca+^{90}Zr has negative Q-values for the transfer of neutrons.

The Coulomb field at large distance for these reactions is the same. The heights of barriers have similar values for these reactions, see Fig. 2. Therefore we may expect that the subbarrier fusion cross sections for these reactions also are similar. However, the experimental subbarrier fusion

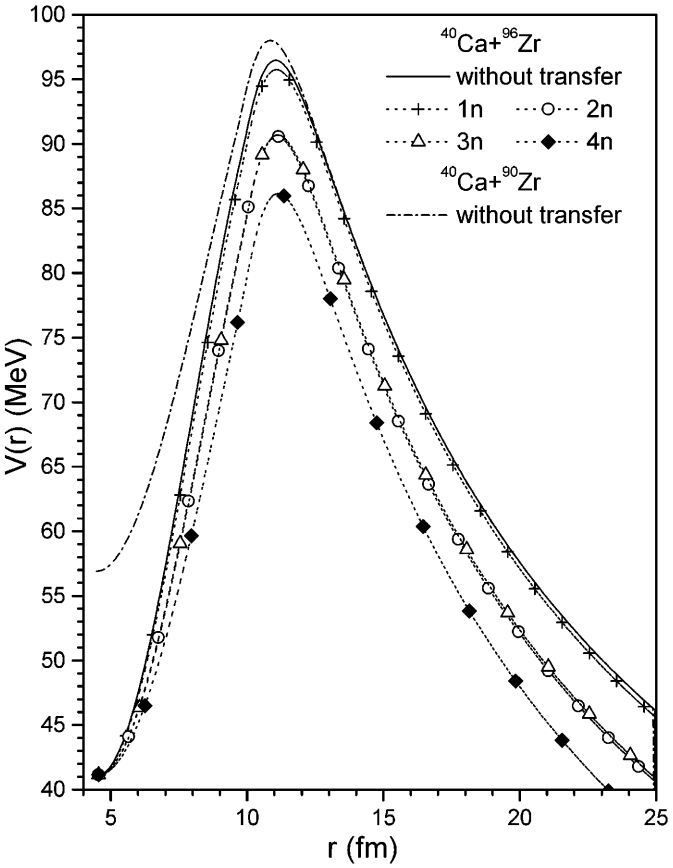

Fig. 2. Effective potential for the reaction ^{40}Ca+^{90,96}Zr for the case $\ell = 0$ and $\epsilon_k = 0$ without and with 1, 2, 3 and 4 neutrons transfer from ^{96}Zr to ^{40}Ca and the effective potential for reactions ^{40}Ca+^{90}Zr without neutron transfer for $\ell = 0$ and $\epsilon_k = 0$

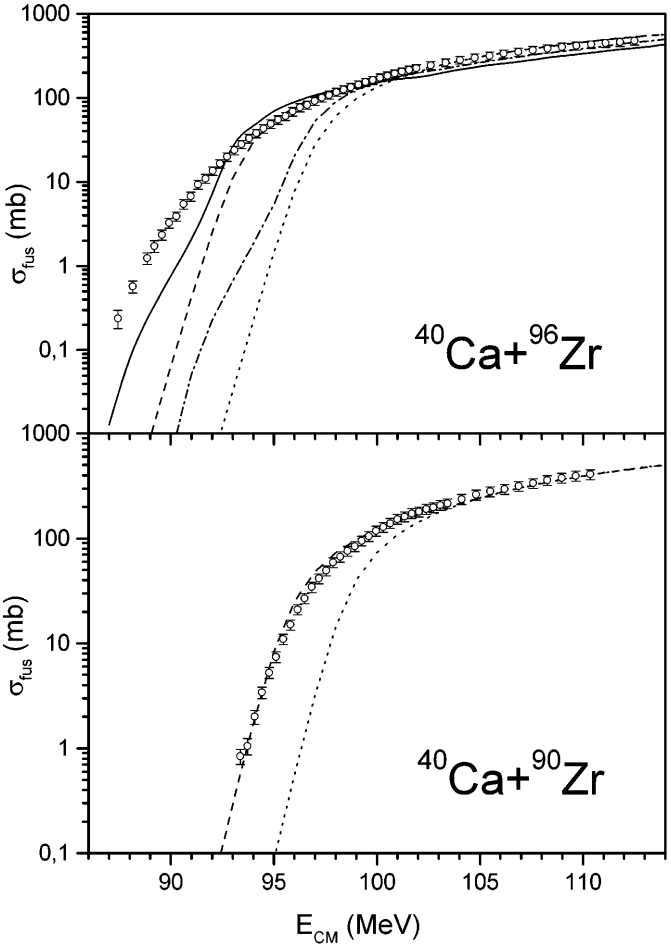

Fig. 3. Fusion cross sections for the reactions ^{40}Ca+^{96}Zr (top) and ^{40}Ca+^{90}Zr (bottom). Experimental data (dots) are taken from [22]. The notations are the same as in Fig. 1

cross sections for the reaction ^{40}Ca+^{96}Zr is much larger than for the reaction ^{40}Ca+^{90}Zr, see Fig. 3 and [22].

At the beginning we try to describe these reactions by using the 1-dimensional WKB approach. The calculations of $\sigma_{\rm fus}(E)$ for both reactions in the one-dimensional tunneling approach yield similar values of the fusion cross sections. But we can see from Fig. 3 that these calculations strongly underestimate the experimental data.

The comparison between the experimental data and the theoretical curves in Fig. 3 is drastically improved for the reaction ^{40}Ca+^{90}Zr when the low-energy surface vibrational 2^+ and 3^- states in colliding nuclei are taken into account. The deformations $\beta_{2,3}$ are taken from another experimental data [53] and are given in Table 1. Nevertheless, the theoretical curves obtained in this approach for reaction ^{40}Ca+^{96}Zr still underestimate the experimental data in Fig. 3.

We performed calculation by taking into account four transfer channels related to 1-, 2-, 3- and 4-neutron transfer from ^{96}Zr to ^{40}Ca. The heights of barriers of the effective potentials related to 2-, 3- and 4-neutron transfer channels are essentially lower then barrier of potential without neutron transfer, see Fig. 2. Therefore we have significant enhancement of the subbarrier fusion cross section by taking into account 2-, 3- and 4-neutron transfer channels. The curves in Fig. 3 associated to this calculation also underestimate the experimental data. Note that the enhancement of subbarrier fusion cross section due to neutron transfer for reaction ^{40}Ca+^{96}Zr in Fig. 3 is much larger than the ones for the reactions Si+Ni in Fig. 1 because of different Q-values of the neutron transfer reactions for this systems. The model describes the experimental data for the reaction ^{40}Ca+^{96}Zr when we take into account the coupling both to the low-energy surface 2^+ and 3^- vibrational states and to the 4 transfer channels, see Fig. 3. This calculation slightly underestimates the experimental fusion cross section ^{40}Ca+^{96}Zr for very low energies. Probably for this reaction it is necessary to take into account the coupling to a larger number of excited surface vibrational states, as done in [22] for reaction ^{40}Ca+^{90}Zr, and to a correlated 2- and 4-neutron transfers.

The reactions ^{40}Ca+^{90,96}Zr are also analyzed in [22] by taking into account the coupling to the 1- and 2-phonon surface vibrational states. The theoretical curves obtained in [22] describe well the experimental data for the ^{40}Ca+^{90}Zr and strongly underestimate the experimental data below barrier for the reaction ^{40}Ca+^{96}Zr.

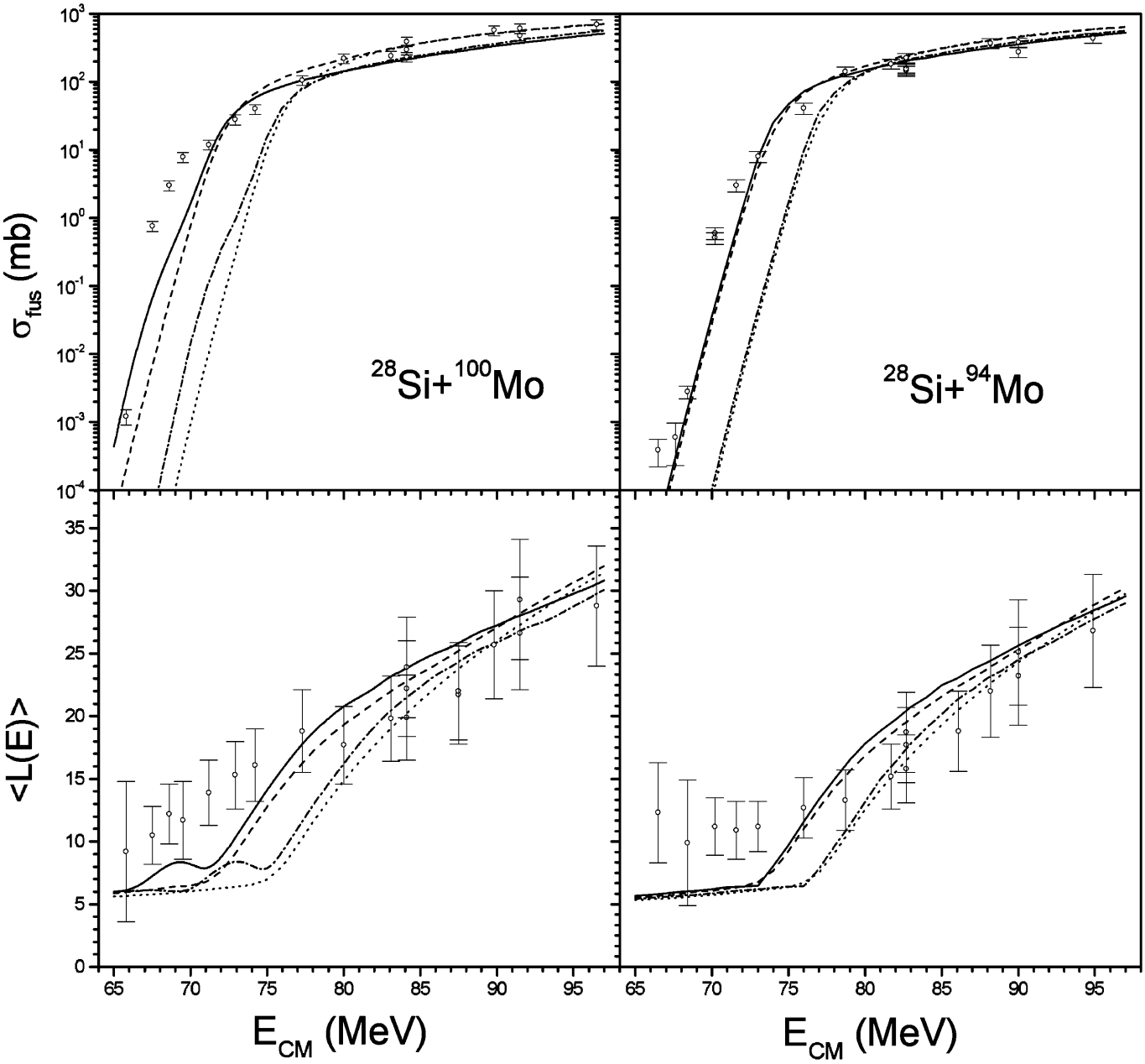

Fig. 4. Fusion cross section (top) and mean angular momentum (bottom) for the reactions ^{28}Si+^{100}Mo (left) and ^{28}Si+^{94}Mo (right). Experimental data (dots) are taken from [32]. The notations are the same as in Fig. 1

Now we consider the fusion reactions ^{28}Si+^{94,100}Mo. We take into account both the low-energy 2^+ and 3^- surface vibrations and the 1-, 2-, 3-, 4-, 5- and 6-neutron transfer channels with positive Q-values in the calculations of the fusion cross sections for ^{28}Si+^{100}Mo. For reaction ^{28}Si+^{94}Mo the coupling to the 2^+ and 3^- surface vibrations and to the 1- and 2-neutron transfer channels with positive Q-values is taken into account in the calculations. The deformations $\beta_{2,3}$ are taken from another experimental data [53] and are listed in Table 1. We can see in Figs. 4 that our calculations describe well the experimental fusion cross sections for the reactions ^{28}Si+^{94,100}Mo [32].

The comparison between the theoretical values and the experimental data for the mean angular momentum $\langle L(E)\rangle = \sum_\ell \ell\sigma(E,\ell)/\sigma(E)$ for the reactions ^{28}Si+^{94,100}Mo is also presented in Fig. 4. The calculation taking into account both the low-energy surface vibrational 2^+ and 3^- states and the transfer channels describes the experimental data for $\langle L(E)\rangle$ for these reactions. The coupling to the transfer channels enhances $\langle L(E)\rangle$ near the barrier and leads to a bump in $\langle L(E)\rangle$ at energies below barrier.

The reactions ^{28}Si+^{94,100}Mo are also analyzed in [32] by taking into account the coupling to the 2^+ and 3^- surface vibrational states and to the 2-neutron trans-

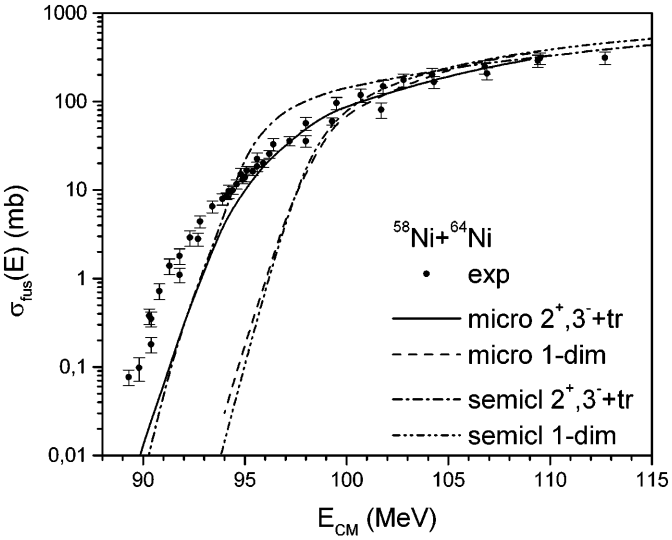

Fig. 5. Fusion cross sections for the reactions ^{58}Ni+^{64}Ni. Experimental data (dots) for reactions ^{58}Ni+^{64}Ni are taken from [32,33]. The results of the calculation taking into account both the low-energy 2^+ and 3^- states and the neutron transfer channels are shown by the solid curve in the case of microscopic coupled channel model [16] and by the dash-dot curve in the case of semiclassical model. The results obtained in the one-dimensional approximation in these models are shown by the dash and the dash-dot-dot curves respectively

fer channel. The 2-neutron transfer channel is treated in [32] phenomenologically. The theoretical curves obtained in [32] also describe well the experimental data for the ^{28}Si+^{94,100}Mo reactions.

The fusion reaction cross section ^{58}Ni+^{64}Ni was measured in [32,33]. The 2-neutron transfer from ^{64}Ni to ^{58}Ni has positive Q-value 3.9 MeV.

The elastic, inelastic, 1n and 2n transfer and fusion reactions in collision ^{58}Ni+^{64}Ni are well described in the framework of the microscopic coupled channel approximation [16]. The microscopic calculation [16] is done by direct solution of the coupled channel equations. The coupling to the neutron transfer channels is very important for this system [16]. Below we analyze the fusion cross section for reaction ^{58}Ni+^{64}Ni in the framework of our semiclassical model. The comparison between the theoretical values obtained in the models and the experimental data for fusion cross section for the reaction ^{58}Ni+^{64}Ni is presented in Fig. 5. Both models describe well the experimental data, as seen in Fig. 5.

We change a little the parameter $r_0 = 1.214$ fm for ^{64}Ni respectively from listed in Table 1 for the sake of coincidence of the fusion cross sections obtained in microscopic and semiclassical calculations in the one-dimensional approximation near and below barrier. In this case we can evaluate the difference between microscopic and semiclassical calculations which originates only from the coupling to both neutron transfer and vibrational states. Using such comparison, we can check the accuracy of our semiclassical approximation.

Comparing results of different calculations in Fig. 5, we may conclude that the semiclassical model agrees well with the detailed microscopical coupled channel calculation. However we should make two comments.

1. The semiclassical model slightly overestimate microscopic calculation at collision energies near barrier (94-98 MeV), as seen in Fig. 5. This take place due to small value of the action at the energies close to 94-98 MeV. It is well-known that the semiclassical approximation has good accuracy in the case of large value of the action or far from the barrier energy [37]. At higher and lower collision energies the difference between semiclassical and microscopic calculations is diminished (see Fig. 5).

2. The cross section evaluated in the one-dimensional microscopic calculation is slightly distinguished from similar semiclassical calculation, as seen in Fig. 5. Therefore, the difference between semiclassical and microscopic calculations in Fig. 5 is not so important, because it may be connected to different parametrizations of the nuclear ion-ion interaction in the models.

The comparison of the theoretical curves with the experimental data in Figs. 1, 3–5 shows that our model describes the entrance channel effects in the subbarrier fusion of a nuclei located along the β-stability line. The neutron transfer channels are very important for the reactions ^{40}Ca+^{96}Zr, ^{28}Si+^{94,100}Mo and ^{58}Ni+^{64}Ni near and especially below barrier, see Figs. 3–5.

4 Subbarrier fusion of nuclei far from the β-stability line

The subbarrier fusion reactions between a nucleus near to the proton drip line and a nucleus near to the neutron drip line should be the most strongly enhanced by the few-nucleon transfer because in this case the separation energies of the transferred particles are small and the Q-values of the transfer reactions have very large positive values. However, it is difficult to perform experiments for such systems. Therefore we study the fusion reaction between a nucleus near to the neutron drip line and a β-stable nucleus in this section. The fusion cross section for such systems may be measured by using radioactive ion beams.

The fusion cross sections for the reactions ^{16,18,20,22,24}O+^{58}Ni obtained in our model are shown in Figs. 6 and 7. The parameters of the low-energy 2^+ and 3^- states for ^{16,18}O and ^{58}Ni taken from [53] are listed in Table 1. The experimental energies of the first 2^+ and 3^- states for the neutron-rich isotope ^{20}O are known [53] but the experimental deformations β_2 and β_3 of these states are not available. Therefore in the calculation we take the same deformations β_2 and β_3 for ^{20}O as for ^{18}O. The experimental data for both energies and the deformation parameters of 2^+ and 3^- states for extremely neutron-rich isotopes ^{22,24}O are absent. Due to this we take the same values of these parameters as for ^{20}O in calculations.

We choose the values of r_0 (see Table 1), diffuseness 0.45 fm of the KNS potential and $\delta = 1.4$ fm for all reac-

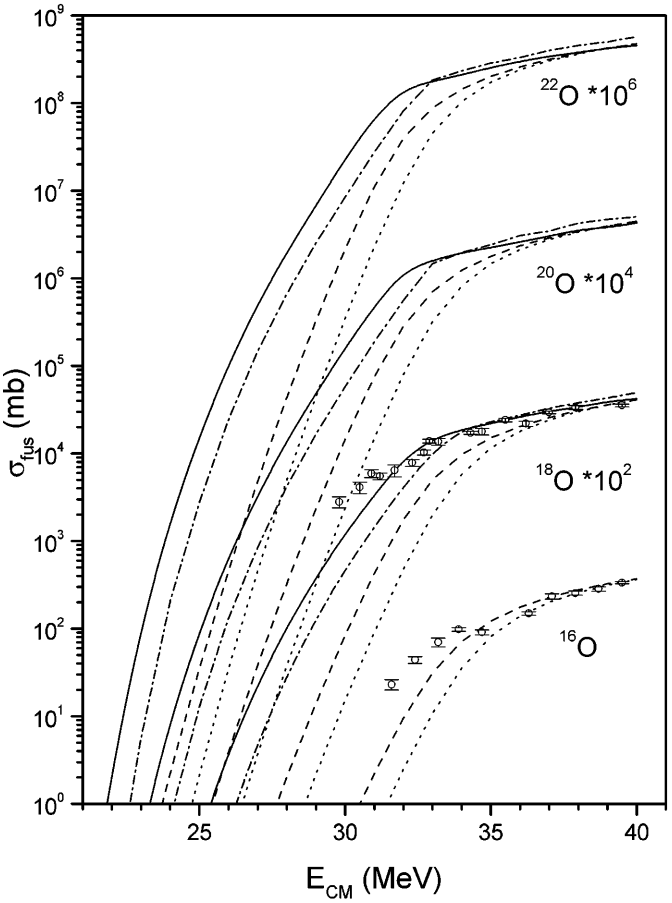

Fig. 6. Fusion cross sections for the reactions ^{16,18,20,22}O+^{58}Ni. Experimental data (dots) for reactions ^{16,18}O+^{58}Ni are taken from [36]. The notations are the same as in Fig. 1

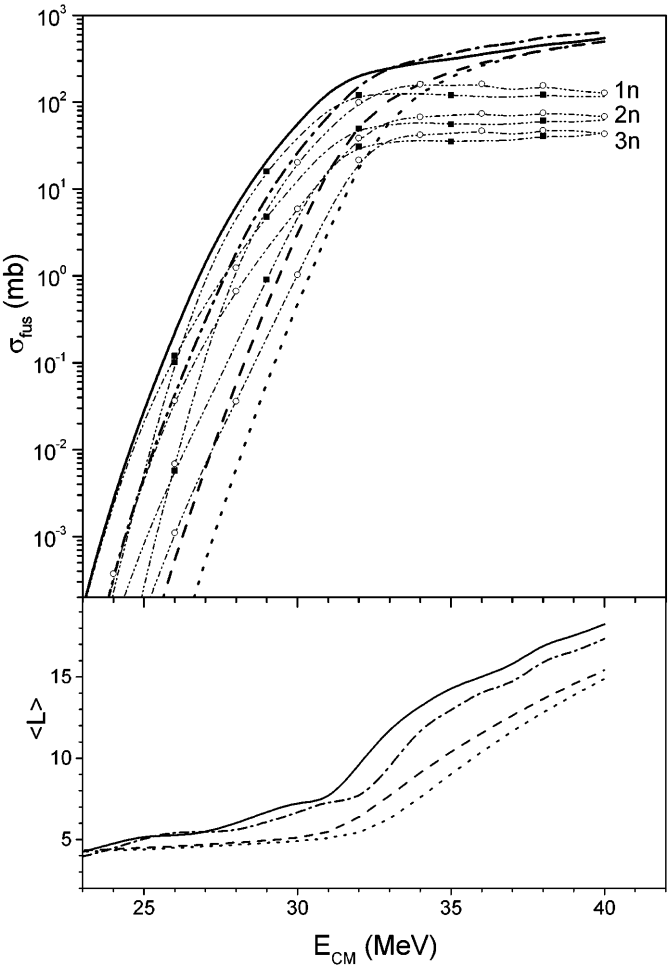

Fig. 7. Fusion cross section (top) and mean angular momentum (bottom) for reaction ^{24}O+^{58}Ni. The partial contributions of channels with 1, 2 and 3 neutrons transfer to the total cross section are marked by filled squares and open ellipses in the cases with and without contributions related to 2^+ and 3^- low-energy excited states, respectively. The other notations are the same as in Fig. 1

tions with oxygen by using the experimental fusion cross section [36] near barrier for the reactions ^{16,18}O+^{58}Ni. (Note that we have taken $\delta = 0.7$ fm for all other reactions discussed above.) The wave functions of the neutrons above the magic number 8 in oxygen isotopes are located in the surface region. Therefore due to the small separation energies of the neutrons in the neutron-rich oxygen isotopes and due to the surface localization of the transferred neutrons the large value of δ is reasonable for these reactions. The value of diffuseness of ion-ion potential for the reactions with oxygen isotopes is smaller then 0.65 fm recommended in [48], but small value of diffuseness of ion-ion potential is often used in the analysis of reactions with light nuclei, (see, for example, [20]). The experimental data for ^{16,18}O+^{58}Ni are well described in the framework of our model, see Fig. 6.

The fusion cross sections for ^{16,18,20,22,24}O+^{58}Ni slightly increase with the number of neutrons for energies near the barrier. The fusion cross sections below barrier are strongly enhanced by the few-neutron transfer from oxygen to nickel. We take into account channels with 1-, 2-, 3- and 4-neutrons transfer in calculations for the reactions ^{18,20,22}O+^{58}Ni. For the reaction ^{24}O+^{58}Ni we employ only three transfer channels related to 1-, 2- and 3-neutron transfer. The influence of few-neutron transfer channels is important below barrier, see Figs 6-7. The enhancement of subbarrier fusion cross section due to neutron transfer channel increases with the number of neutrons in oxygen.

The partial contributions of the channels with 1-, 2- and 3-neutron transfer to the total fusion cross sections ^{24}O+^{58}Ni are shown in Fig. 7. We may conclude that the 1-neutron transfer channel is important for energies near the barrier, the 2-neutron transfer channel gives dominant contributions for low energies and the 3-neutron transfer channel give small contributions for energies larger than 23 MeV.

The energy dependence of the mean angular momentum $\langle L(E) \rangle$ of the compound nucleus formed in the fusion reaction ^{24}O+^{58}Ni in different approaches is shown in Fig. 7. We can see in Fig. 7 that the 1-neutron transfer

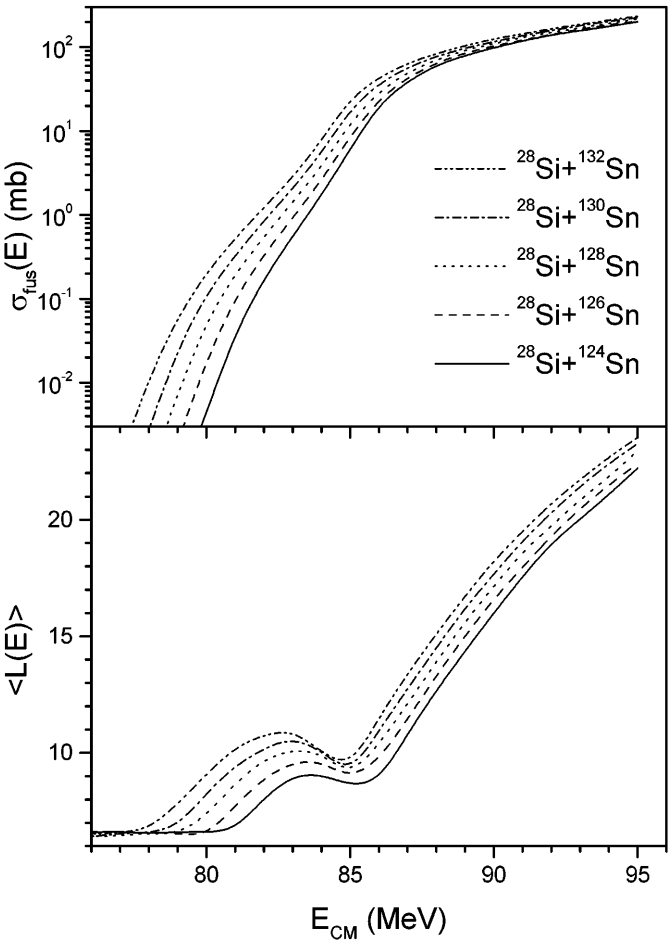

Fig. 8. Fusion cross section (top) and mean angular momentum (bottom) for the reactions ^{28}Si+^{124,126,128,130,132}Sn

channel enhances $\langle L(E)\rangle$ near barrier and the 2-neutron transfer channel leads to the maximum in $\langle L(E)\rangle$ at subbarrier energies.

Note that the fusion cross sections for systems ^{24}O+^{58}Ni and ^{40}Ca+^{96}Zr have different behaviors near barrier due to the 1-neutron transfer channel contribution. This channel is not important for the reaction ^{40}Ca+^{96}Zr in contrast to the reaction ^{24}O+^{58}Ni. Such difference is related to the Q-values of the 1-neutron transfer channel for these reactions: $Q_{1n} = 5.29$ MeV for ^{24}O+^{58}Ni and $Q_{1n} = 0.508$ MeV for ^{40}Ca+^{96}Zr.

The energy dependence of the fusion cross sections and of the mean angular momentum for the reactions ^{28}Si+^{124,126,128,130,132}Sn are presented in Fig. 8. In the calculations we take into account both the 1-, 2-, 3- and 4-neutron transfer channels from the tin isotopes to silicon and the coupling to 2^+ and 3^- low-energy states. We see in Fig. 8 that $\sigma_{\rm fus}(E)$ and $\langle L(E)\rangle$ increase drastically with the number of neutrons in the tin isotopes due to the two-neutron transfer below barrier.

Our calculation of $\sigma_{\rm fus}(E)$ and $\langle L(E)\rangle$ for the reactions ^{28}Si+^{124,126,128,130,132}Sn is done for $\delta = 0.7$ fm, because the ^{132}Sn is a double magic nucleus. The values of the parameters of the 2^+ and 3^- low-energy states and the radii r_0 in the KNS potential are listed in Table 1. Note that in the case of tin isotopes we know the values of the energies and the deformation parameters $\beta_{2,3}$ of the 2^+ and 3^- states for ^{124}Sn only, see [53]. The experimental deformations $\beta_{2,3}$ for the isotopes ^{126,128,130,132}Sn are not known [53]. Therefore we take the same values of β_2 and β_3 for these isotopes as for ^{124}Sn. The energies of the 2^+ and 3^- states in ^{124,126,128,130}Sn are located around 1.1-1.2 MeV and 2.5-2.8 MeV, respectively [53]. The known experimental energies of the first 2^+ and 3^- states in ^{132}Sn [53] are higher than the corresponding ranges of energies of the first 2^+ and 3^- states in ^{124,126,128,130}Sn. For the reason of systematic of the excitation energies in the tin isotopes we take the same energies of the 2^+ and 3^- states for ^{132}Sn as for ^{130}Sn.

5 Conclusions

We have analyzed the subbarrier fusion cross sections, the mean and angular momentum induced by heavy ions collisions. The coupling to the low-energy surface vibrational states and to the subbarrier few-neutron transfer channels are taken into account in our model.

It is shown that the few-nucleon transfer with a large positive Q-value leads to strong enhancement of $\sigma_{\rm fus}(E)$ and $\langle L(E)\rangle$. Due to few-nucleon transfer the slope of the fusion cross section changes and a non-monotonous energy dependence appears in $\langle L(E)\rangle$.

The few-nucleon transfer enhancement of subbarrier fusion reactions is very important for the case of systems with small separation energies of the transferred particles and with large positive Q-value of the transfer reactions. The favorable conditions for this enhancement take place in reactions between a nucleus near the neutron drip line and a nucleus along the line of β-stability. As a rule, the most important contributions to the few-nucleon transfer enhancement of the subbarrier fusion are related to the 1- and 2-nucleon transfer channels.

Our model has been applied to the few-neutron transfer case in this paper. The inclusion of few-proton transfer in our model is direct because it is necessary to take into account the Coulomb interactions between the ions and the transferred protons in the action (13). An extension of our model to the case of neutron-proton transfer is also straightforward but the sequence of the neutron-proton transfer should be taken into account due to the different values of the separation energies of nucleons for different sequences of neutron-proton transfer.

Our calculation is based on the parameterization (18) of the ion-ion interaction at small distance. The parameterization (18) is matched with the Coulomb and the KNS nuclear interactions in Sec. 2. Note that this parameterization may be matched with any other potentials and may be used for the description of other reactions near the barrier.

We consider sequential transfer of neutrons. This transfer mechanism is may apply for colliding nuclei located not very far from β-stability line. For extremely far

from the β-stability line colliding nuclei probably is necessary to take into account correlated transfer of neutrons [8]. The correlated neutron transfer may be especially important in the case of fusing system with two-neutron halo nucleus. It is possible to consider correlated transfer of neutrons in the framework of the model also if we change the action (13) correspondingly.

The author would like to thank R.W. Hasse and F.A. Ivanyuk for careful reading of manuscript. He acknowledges gratefully support from GSI. He also would likes to thank A.M. Stefanini for bringing the Table of experimental data measured in [22] to his attention before publication.

6 Appendix

We derived expression (8)–(13) by using the path integral representation of the quantum mechanics amplitude [54].

The amplitude of transition through the barrier in the case of two variables is connected with the path integral [54]

$$\langle R_f, r_f | R_i, r_i \rangle = \int \mathcal{D}R(t)\, \mathcal{D}r(t)\, \exp\left(i\mathcal{S}[R,r]/\hbar\right), \quad \text{(A.1)}$$

where $\mathcal{S}[R,r]$ is the action. Variables r and R are associated with the coordinates of relative motion of the ions and the transferred neutron respectively. The coordinates with indexes $i(f)$ are related to the initial (final) turning point.

By using the properties of the path integral [54], we rewrite the amplitude in the form

$$\begin{aligned}&\langle R_f, r_f | R_i, r_i \rangle \\ &= \int \mathcal{D}R_1(t)\, \mathcal{D}r_1(t) \mathcal{D}R_2(t)\, \mathcal{D}r_2(t)\, \langle R_f, r_f | R_2, r_2 \rangle \\ &\quad \langle R_2, r_2 | R_1, r_1 \rangle \langle R_1, r_1 | R_i, r_i \rangle. \end{aligned} \quad \text{(A.2)}$$

The velocity of transferred neutron is related to the Fermi energy. At low collision energies the velocity of transferred neutron is much higher then the relative velocity of ions at small distance between them in classical allowed region. Due to this and large difference between the neutron mass and the ions' reduced mass μ, we may consider that in the classical forbidden region the collective degree of freedom r is much slower then single-particle R. Let us assume that the transfer of neutrons takes place in the path between (R_1, r_1) and (R_2, r_2). The transfer is fast process in comparison with ions motion, and we can consider the neutron transfer in the instantaneous limit $r_1 \to r_2 = r_{\rm tr}$. The transition amplitude (A.2) for the ions' barrier penetration in this limit is presented as

$$\begin{aligned}\langle R_f, r_f | R_i, r_i \rangle = \int \mathcal{D}r_{\rm tr}(t)\, \langle R_f, r_f | R_f, r_{\rm tr} \rangle \\ \times \langle R_f, r_{\rm tr} | R_i, r_{\rm tr} \rangle\, \langle R_i, r_{\rm tr} | R_i, r_i \rangle. \end{aligned} \quad \text{(A.3)}$$

Notice that since the paths are weighted with $\exp(\mathcal{S})$ (A.1), important contribution to the transition amplitude are expected to arise from those paths for which $\mathcal{S}$ takes values close to the minimum. It leads us to the principle of the minimal action used in section 2.

The path integral and the Schrödinger representations of the transition amplitude are equivalent [54]. By using the semiclassical approximation for the transition amplitude in the classically forbidden region in the Schrödinger representation [37], we present square of the amplitude (or transmission coefficient (8)) in the form

$$\begin{aligned}&|\langle R_f, r_f | R_i, r_i \rangle|^2 \\ &\approx |\exp[-2i/\hbar(\mathcal{S}_i[R_i, r_i, r_{\rm tr}] + \mathcal{S}_{\rm tr}[R_i, R_f, r_{\rm tr}] \\ &\quad + \mathcal{S}_f[R_f, r_{\rm tr}, r_f])]| \\ &= \exp\left[-\mathcal{A}^i(E, \mathcal{V}^i_{\ell k}, r_{\rm tr}) - \mathcal{A}^{\rm tr}(E, r_{\rm tr}) - \mathcal{A}^f(E, \mathcal{V}^f_{\ell k}, r_{\rm tr})\right], \end{aligned} \quad \text{(A.4)}$$

where $r_{\rm tr}$ is obtained using the principle of the minimal action, and the actions $\mathcal{A}$ are presented by expressions (10), (11) and (13).

We obtain expression (13), if we suggest that the transfer of m neutrons also occurs sequentially at the same point $r_{\rm tr}$ as transfer of the first transferred neutron.

The (8) and (A.4) coincides one with another with the exponential accuracy. We use in our calculations (8), because the expression (8) for transmission coefficient coincides with one-dimensional transmission coefficient [55], if the neutron transfer in the course of barrier penetration is neglected.

References

1. R. Bass, *Nuclear Reaction with Heavy Ions*, (Springer-Verlag, Berlin 1980)
2. L.C. Vaz, J.M. Alexander, G.R. Satchler, Phys. Rep. **69**, 373 (1981)
3. M. Beckerman, Phys. Rep. 129 (1985) 145; Rep. Prog. Phys. **51**, 1047 (1988)
4. S.G. Steadman, M. J. Rhoades-Brown, Ann. Rev. Nucl. Part. Sci. **36**, 649 (1986)
5. V.P. Permyakov, V.M. Shilov, Sov. J. Part. Nucl. **20**, 594 (1989)
6. G.R. Satchler, Phys. Rep. **199**, 147 (1991)
7. R. Vandenbosch, Ann. Rev. Nucl. Part. Sci. **42**, 447 (1992)
8. W. Reisdorf, J. Phys. G**20**, 1297 (1994)
9. A.M. Stefanini, Nucl. Phys. A**538**, 195c (1992); J. Phys. G**23**, 1401 (1997)
10. A.B. Balantekin, N. Takigawa, Rev. Mod. Phys. **70**, 77 (1998)
11. V.M. Shilov, A.V. Tarakanov, Phys. At. Nucl. **56**, 741 (1993)
12. N. Rowley, Nucl.Phys. A**630**, 67c (1998)
13. C.H. Dasso, S. Landowne, Comp. Phys. Comm. **46**, 187 (1987)
14. R.A. Broglia, C.H. Dasso, S. Landowne, G. Pollarolo, Phys. Lett. B**133**, 34 (1983)
15. A. Winther, Nucl. Phys. A**572**, 191 (1994); Nucl. Phys. A**594**, 203 (1995).

16. H. Esbensen, S. Landowne, Nucl. Phys. A**492**, 473 (1989); A.M. Stefanini, J. Xu, L. Corradi, G. Montagnoli, H. Moreno, Y. Nagashima, L. Mueller, M. Narayanasamy, D.R. Napoli, P. Spolaole, S. Beghini, F. Scarlassara, G.F. Segato, F. Soramel, C. Signorini, H. Esbensen, S. Landowne, G. Pollarolo, Phys. Lett. B**240**, 306 (1990)
17. R.A. Broglia, C.H. Dasso, S. Landowne, A. Winther, Phys. Rev. C**27**, 2433 (1983)
18. L. Corradi, S.J. Skorka, T. Winkelmann, K. Balog, P. Janker, H. Leitz, U. Lenz, K.E.G. Lobner, K. Rudolf, M. Steinmayer, H.G. Thies, B. Millon, D.R. Napoli, A.M. Stefanini, S. Beghini, G. Montagnoli, F. Scarlassara, C. Signorini, F. Soramel, Z. Phys. A**346**, 217 (1993)
19. L. Corradi, in *Proc. Workshop on heavy ion fusion: exploring the variety of nuclear properties, Padova, Italy, 1994*, edited by A.M. Stefanini et al. (World Scientific, Singapore 1994) p. 34
20. B. Imanishi, V. Denisov, T. Motobayashi, Phys. Rev. C**55**, 1946 (1997); B. Imanishi, V. Denisov, in *Proc. Int. School-Seminar on Nuclear Structure and Related Topics, Dubna, September 1997*, (in press)
21. A.M. Stefanini, D. Ackermann, L.Corradi, J.H. He, G. Montagnoli, S. Beghini, F. Scarlassara, G.F. Segato, Phys. Rev. C**52**, R1727 (1995)
22. H. Timmers, D. Ackermann, S. Beghini, L. Corradi, J.H. He, G. Montagnoli, F. Scarlassara, A.M. Stefanini, N. Rowley, Nucl. Phys. A**633**, 421 (1998)
23. P.R.S. Gomes, A.M.M. Maciel, R.M. Anjos, S.B. Moraes, R. Liguori Neto, R. Cabezas, C. Muri, G.M. Santos, J.F. Liang, J. Phys. G**23**, 1315 (1997)
24. M. Dasgupta, et al., in *Proc. Workshop on heavy ion fusion: exploring the variety of nuclear properties, Padova, Italy, 1994*, edited by A.M. Stefanini et al. (World Scientific, Singapore 1994) p. 115
25. S. Gil, in *Proc. Workshop on heavy ion fusion: exploring the variety of nuclear properties, Padova, Italy, 1994*, edited by A.M. Stefanini et al. (World Scientific, Singapore 1994) p. 78
26. V.Yu. Denisov, Sov. J. Nucl. Phys. **54**, 952 (1991); V.Yu. Denisov, G. Royer, J. Phys. G**20**, L43 (1994); V.Yu. Denisov, G. Royer, Phys. At. Nucl. **58**, 397 (1995); V.Yu. Denisov, S.V. Reshitko, Phys. At. Nucl. **59**, 78 (1996)
27. J. Schneider, H.H. Wolter, Z. Phys. A**339**, 177 (1991)
28. C.E. Aguiar, V.C. Barbosa, L.F. Canto, R. Donangelo, Nucl. Phys. A**472**, 571 (1987)
29. R. Pengo, D. Evers, K.E.G. Lobner, U. Quade, K. Rudolph, S.J. Skorka, I. Weidl, Nucl. Phys. A**411**, 255 (1983)
30. H.-J. Hennrich, G. Breitbach, W. Kuhl, V. Metag R. Novotny, D. Habs, D. Schwalm, Phys. Lett. B**258**, 275 (1991)
31. A.M. Stefanini, G. Fortuna, R. Pengo, W. Meczynski, G. Montagnoli, L. Corradi, A. Tivelli, S. Bechini, C. Signorini, S. Lunardi, M. Morando, and F. Soramel, Nucl. Phys. A**456**, 509 (1986)
32. D. Ackermann, P. Bednarczyk, L. Corradi, D.R. Napoli, C.M. Petrache, S. Spolaore, A.M. Stefanini, K.M. Varier, H. Zhang, F. Scarlassara, S. Beghini, G. Montagnoli, L. Müller, G.F. Segato, F. Soramel, C. Signorini, Nucl. Phys. A**609**, 91 (1996)
33. M. Beckerman, M. Salomaa, A. Sperduto, J.D. Molitoris, A. DiRienzo, Phys. Rev. C**25**, 837 (1982)
34. C. Signorini, Nucl. Phys. A**616**, 262c (1997)
35. K.E. Rehm, Annu. Rev. Nucl. Part. Sci. **41**, 429 (1991)
36. A.M. Borges, C.P. da Silva, D. Pereira, L.C. Chamon, E.S. Rossi, C.E. Aguiar, Phys. Rev. C**46**, 2360 (1992)
37. L.D. Landau, E.M. Lifshits, *Quantum mechanics. Nonrelativistic theory* (Pergamon Press, Oxford 1977).
38. R.A. Broglia, G. Pollarolo, A. Winther, Nucl. Phys. A**361**, 307 (1981); G. Pollarolo, R.A. Broglia, A. Winther, Nucl. Phys. A**406**, 369 (1983).
39. W. von Oertzen, H.G. Bohlen, B. Gebauer, R. Kinkel, F. Puhlhofer, D. Schull, Z. Phys. A**326**, 463 (1987).
40. M. Devlin, D. Cline, R. Ibbotson, M.W. Simon, C.Y. Wu, Phys. Rev. C**53**, 2900 (1996)
41. L. Corradi, J.H. He, D. Ackermann, A.M. Stefanini, A. Pisent, S. Beghini, G. Montagnoli, F. Scarlassara, G.F. Segato, G. Pollarolo, C.H. Dasso, A. Winther Phys. Rev. C**54**, 201 (1996)
42. J.F. Liang, L.L. Lee, J.C. Mahon, R.J. Vojtech, Phys. Rev. C**50**, 1550 (1994)
43. K.E. Rehm, C.L. Jiang, J. Gehring, B. Glagola, W. Kutschera, M.D. Rhein, A.H. Wuosmaa, Nucl. Phys. A**583**, 421c (1995)
44. C.L. Jiang, K.E. Rehm, H. Esbensen, D.J. Blumenthal, B. Crowell, J. Gehring, B. Glagola, J.P. Schiffer, A.H. Wuosmaa, Phys. Rev. C**57**, 2393 (1998)
45. D.L. Hill, J.A. Wheeler, Phys. Rev. **89**, 1102 (1953)
46. A. Bohr, B. Mottelson, Nuclear Structure, vol. 1 (Benjamin Press, Reading, MA, 1969).
47. WWW page *http* : *//www − nds.iaea.or.at/ripl/*, file beijing_bs.dat
48. H.J. Krappe, J.R. Nix, A.J. Sierk, Phys. Rev. C**20**, 992 (1979)
49. G. Audi, A.H. Wapstra, Nucl. Phys. A**595**, 409 (1995)
50. P. Möller, J.R. Nix, Nucl. Phys. A**361**, 117 (1981)
51. P. Möller, J.R. Nix, W.J. Swiatecki, Nucl.Phys. A**492**, 349 (1989)
52. G. Royer, R.K. Gupta, V. Denisov, Nucl. Phys. A**632**, 275 (1998)
53. K.I. Pearce, N.M. Clarke, R.J. Griffiths, P.J. Simmonds, D. Barker, J.B. A. England, M.C. Mannion, C.A. Ogilvie, Nucl. Phys. A**467**, 215 (1987); M.M. King, Nucl. Data Sheets **60**, 337 (1990); H.F. Lutz, D.W. Heikkinen, W. Bartolini, Phys. Rev. C**4**, 934 (1971); M. Lahanas, D. Rychel, P.Singh, R. Gyufko, D. Kolbert, B. van Kruchyen, E. Hadadakis, C.A. Wiedner, Nucl. Phys. A**455**, 399 (1986); C.R. Gruhn, T.Y.T. Kuo, C.J. Maggiore, H. McManus, F. Petrovich, B.M. Preedom, Phys. Rev. C**6**, 915 (1972); P. Grabmayer, J. Rapaport, R.W. Finlay, Nucl. Phys. A**350**, 167 (1980); T. Tamura, K. Miyama, S. Ohya, Nucl. Data Sheets **41**, 414 (1984); T. Tamura, K. Miyama, S. Ohya, Nucl. Data Sheets **36**, 227 (1982); K. Kitao, M. Kanbe, Z. Matumoto, Nucl. Data Sheets **38**, 191 (1983); Yu. V. Sergeenkov, Nucl. Data Sheets **58**, 765 (1989); Yu.V. Sergeenkov, Nucl. Data Sheets **65**, 277 (1992)
54. R.P. Feynman, A.R. Hibbs, *Quantum Mechanics and Path Integrals*, (McGraw-Hill Inc., New York 1965).
55. N. Fröman, P.O. Fröman, *JWKB Approximation*, (North-Holland Publ. Co., Amsterdam 1965).